Brazilian Dental Science

unesp
UNIVERSIDADE ESTADUAL PAULISTA
"JÚLIO DE MESQUITA FILHO"
Instituto de Ciência e Tecnologia
Campus de São José dos Campos

ORIGINAL ARTICLE

DOI: https://doi.org/10.4322/bds.2024.e4552

Antibacterial and remineralizing effects of orthodontic adhesive modified by nano-chitosan loaded with calcium phosphate

Efeitos antibacteriano e remineralizante de adesivo ortodôntico modificado com nanopartículas de quitosana carregadas com fosfato de cálcio

Lara Riyadh AL-BANAA[1], **Ali R. AL-KHATIB**[1], **Fawzi Habeeb JABRAIL**[2]

1 - Mosul University, College of Dentistry, Department of Pedodontics, Orthodontic and Preventive Dentistry. Mosul, Iraq.
2 - Mosul University, College of Science, Department of Chemistry. Mosul, Iraq.

How to cite: Al-Banaa LR, Al-Khatib AR, Jabrail FH. Antibacterial and remineralizing effects of orthodontic adhesive modified by nano-chitosan loaded with calcium phosphate. Braz Dent Sci. 2024;27(4):e4552. https://doi.org/10.4322/bds.2024.e4552

ABSTRACT

Objective: The objective of this study was to evaluate the remineralizing and antibacterial effects of orthodontic adhesive modified with nano-chitosan loaded with calcium phosphate, and to investigate the adhesive's physical and chemical properties. **Material and Methods:** Transbond™ XT adhesive primer was modified by nano-chitosan loaded with calcium phosphate, this study compared three groups: Control primer without any additive, 5% and 10% nano-chitosan/ calcium phosphate primer in terms of Fourier Transform Infrared Spectrometer, Shear Bond Strength, Degree of monomer Conversion, Contact Angle measurement, Antibacterial properties against *Streptococcus mutans* and *Lactobacillus acidophilus*, and Field Emission Scanning Electron Microscopy with Energy Dispersive X-ray Spectroscopy to examine remineralization of the demineralized enamel. Statistical Analysis used to compare the results using descriptive statistics, one-way ANOVA, and Tukey's post hoc test. Statistical significance was set at $P<0.05\%$. **Results**: Both 5% and 10% nano-chitosan/ calcium phosphate primer showed significant increases in the SBS, DC, antibacterial, and remineralization of demineralized enamel (higher mineral contents and greater Ca/P ratio) when compared to the control group. Contact angle values showed non-significant differences among groups. **Conclusion:** The orthodontic adhesive primer modified with nano-chitosan/ calcium phosphate showed improved physical, chemical, and biological properties including enhanced antibacterial and remineralization compared to the commercial non modified adhesive primer. The 10% nano-chitosan/ calcium phosphate primer group displayed superior improvements across all the tested adhesive properties compared to the control and 5% nano-chitosan/ calcium phosphate primer groups.

KEYWORDS

Calcium phosphate; Chitosan; Degree of conversion; Orthodontic adhesive; Remineralization.

RESUMO

Objetivo: O objetivo deste estudo foi avaliar o efeito remineralizante e antibacteriano de um adesivo ortodôntico modificado com nanopartículas de quitosana carregadas com fosfato de cálcio, e investigar as propriedades físicas e químicas do adesivo. **Material e Métodos:** O primer do adesivo Transbond™ XT foi modificado com nanopartículas de quitosana carregadas com fosfato de cálcio, comparando três grupos: Primer controle sem aditivos; Primer contendo 5% e 10% de nanopartículas de quitosana/fosfato de cálcio; em relação a espectroscopia no infravermelho por transformada de Fourier, resistência ao cisalhamento, grau de conversão dos monômeros, mensuração do ângulo de contato, propriedades antibacterianas contra Streptococcus mutans e Lactobacillus acidophilus, e microscopia eletrônica de varredura com emissão por campo para examinar a remineralização do esmalte desmineralizado. A análise estatística foi usada para comparar os valores obtidos na estatística descritiva, com ANOVA um fator e teste de Tukey. O nível de significância adotado foi $p<0,05\%$. **Resultados:**

Ambos os primers contendo 5% e 10% de nanopartículas de quitosana/fosfato de cálcio mostraram aumento significante em relação à resistência ao cisalhamento, grau de conversão, ação antibacteriana e remineralização do esmalte (alto conteúdo mineral e maior relação Ca/P) quando comparado ao grupo controle. Os valores do ângulo de contato mostraram-se sem diferenças significantes entre os grupos. **Conclusão:** O primer do adesivo ortodôntico modificado com nanopartículas de quitosana carregadas com fosfato de cálcio mostrou melhores propriedades físicas, químicas e biológicas, incluindo melhora antibacteriana comparada ao primer comercial não modificado. O primer contendo 10% de nanopartículas de quitosana/fosfato de cálcio mostrou melhores resultados comparado ao controle e o primer contendo 5%.

PALAVRAS-CHAVE

Fosfato de cálcio; Quitosana; Grau de conversão; Adesivo ortodôntico; Remineralização.

INTRODUCTION

White spot lesions (WSLs) are the initial clinical signs of enamel demineralization that can progress into cavitated lesions with gradual dissolution of the enamel hydroxyapatite crystals and loss of tooth tissue [1,2]. WSLs are classified according to Nyvad et al. [3] criteria in to: Active lesion, characterized by a whitish or yellowish rough chalky surface with loss of luster; feels rough when the tip of the probe is moved gently across the surface; or inactive lesion, if they have a smooth shiny surface and feels hard and smooth when the tip of the probe is moved gently across the surface.

Two types of bacteria are involved in tooth decay; *Streptococcus mutans* which is primarily responsible for initiating dental caries, and *Lactobacillus acidophilius*, which contributes to the development and progression of caries pathogenesis [4]. Both bacteria can produce acid during the metabolism of sugar fermentation. The acid produced in the dental plaque on tooth surface readily diffuse in all directions in the mouth, it also diffuses into the pores of enamel and begins to dissolve it. In the mouth, this process progresses long enough; the result is a cavity. This process usually takes several months to years for progression to cavitation, the end-point of the disease process known as dental caries [5].

The remineralization mechanism is a natural repairing process that occurs under a neutral physiological pH condition, it restores the ionic forms of the minerals to the hydroxyapatite crystal lattice (HAP). Plaque and saliva are sources of calcium and phosphate ions which precipitate into the demineralized enamel lesion forming larger HAP crystals with greater resistance to acid dissolution [6]. Various types of remineralizing agents are used, they are classified into fluorides and non-fluoride agents. Calcium phosphate materials are non-fluoride remineralizing agents and the main components of HAP crystals [7].

Calcium phosphate, considered a source of Ca^{+2} and PO_4^{-3} ions, is used to improve the saturation of HAP in early carious lesions. In nature, there are various types of calcium phosphate compounds which include: Tri Calcium Phosphate, Tetra Calcium Phosphate, Amorphous Calcium Phosphate (ACP), Octa Calcium Phosphate, Mono Calcium Phosphate Monohydrate, and HAP [8].

Combining remineralizing agents with antibacterial strategies can enhance their effectiveness in treatment of WSL. It might be beneficial to combine remineralization systems such as calcium phosphate with natural antibacterial agents, like chitosan.

Chitosan is a natural carbohydrate polymer prepared by the de-N-acetylation of chitin, which is the main component of the exoskeleton of insects, shrimps, and crustaceans [9]. It has been incorporated in to various dental products, including composite resin, glass ionomer cement, and many adhesive materials, for improving mechanical and antibacterial properties because it is biocompatible, has antioxidant activity and exhibits no toxicity [10].

Chitosan is useful in preventing dental caries for several reasons: (i) it has adhesive property so in acidic media, chitosan's amino groups become protonated, resulting in positively charged molecules that adhere to negatively charged surfaces such as cell membranes and tooth enamel [11]; (ii) it possesses antibacterial activity. Its mechanism involves interaction with bacterial cell wall, promoting the displacement of Ca^{++} from anionic membrane sites, leading to cellular destruction [12]; (ii) It inhibits demineralization by acting as a barrier against

acid penetration (iii) it prevents phosphorus release from the enamel [13]; (iiii) The structure of chitosan acts as a drug delivery system as it has specialized active regions that combine with various bioactive materials to release ions required for remineralization [9,14]. Chitosan has been applied as a composite agent in the formation of hybrid materials with calcium phosphates, which are widely used for dental restorations and bone tissue regeneration [15]. Several hybrid remineralizing agents combining chitosan and calcium phosphates have been evaluated, including: hybrid Chitosan-Hydroxyapatite [16], Carboxymethyl chitosan- Amorphous Calcium Phosphate nanocomplexes [17], Chitosan/ Calcium Pyrophosphate microflowers [18], etc.

Previous studies analyses showed that no studies have investigated the biological properties of adding nano chitosan loaded with calcium phosphate to an orthodontic primer. Therefore, the current study aimed to evaluate the effect of adding nano- chitosan loaded with calcium phosphate as an antibacterial and remineralizing agent while maintaining acceptable physical and chemical properties of the orthodontic adhesive.

The null hypothesis assumed that modification of the orthodontic adhesive primer has no effect on the remineralizing, antimicrobial, physical, and chemical properties of the orthodontic adhesive.

MATERIAL AND METHODS

The University of Mosul, College of Dentistry's ethics committee approved this study on February 5, 2023, with the reference number (UoM.Dent. 23/24).

The materials used in this study included:

1. Nano-chitosan powder (Nanochemazone Company, Canada) with particles size range between 30-50 nm, molecular formula ($C_6H_{11}NO_4$), purity 99.9%, and molecular weight of 161 g/mol;
2. Tricalcium Phosphate (Sigma-Aldrich Germany) with the chemical formula $Ca_3(PO_4)_2$, molecular weight: 310.18, and assay analysis ≥98% β-phase basis (sintered Powder);
3. Transbond XT primer (3M Unitek, Monrovia, USA) was used in the study.

Preparation of nano-chitosan solution loaded with calcium phosphate

1.0 g of nano-chitosan powder was dissolved in 100 mL of deionized distilled water containing 1 mL of 2% (v/v) acetic acid solution (Merck KGaA, Darmstadt, Germany), The mixture was stirred using magnetic stirring for approximately three hours at room temperature to achieve a homogenous nano-chitosan solution. The pH of the dissolved chitosan solution was adjusted to 7.0 by adding a 0.05 M dropwise of NaOH solution [19].

Nano-chitosan loaded with calcium phosphate solution was prepared by mixing chitosan with calcium phosphate in a 5:1 weight ratio. Specifically, 200mg of calcium phosphate powder was added to the chitosan solution under magnetic stirring for 3 hours at room temperature.

Preparation of the modified orthodontic primer

This study compared three groups, as shown in Table I. To prepare 0%, 5%, and 10% nano-chitosan/calcium phosphate modified primer (ChCPP) in weight-to-weight ratios, one drop (50 μl in size) of primer was measured using a micropipette (10-100 μm) for standardization. A digital scale was used to weigh one drop which was equivalent to 0.05 g, for each group, 20 drops of modified primer were prepared by mixing 1 g of primer with 0.05, and 0.1 g of nano-chitosan/calcium phosphate to prepare 5% ChCPP, and 10% ChCPP groups respectively, along with a control group. Mixing was done in a semi-dark environment inside microtubes by

Table I - Groups of the study

No.	Name	Description
1	Control	No additive
2	5% ChCPP	5% Chitosan loaded with Calcium Phosphate modified Primer
3	10% ChCPP	10% Chitosan loaded with Calcium Phosphate modified Primer

ChCPP: Chitosan/Calcium Phosphate Primer.

using the straight head of a dental probe until a uniform consistency was achieved. Furthermore, an ultrasonic bath was used to enhance the distribution of the material into the primer for 30 min. The microtubes were wrapped in dark tape to prevent light exposure, the method of modified primer preparation followed that of Nader et al. [20].

Testing procedures

Field Emission Scanning Electron Microscopy and Energy Dispersive X-ray spectroscopy (FESEM-EDX) characterization of nano-chitosan/calcium phosphate

The morphology and distribution of calcium phosphate particles within the nano-chitosan solution were frozen by liquid nitrogen and then analyzed using Field Emission Scanning Electron Microscopy(FESEM) at 20 kV accelerating voltage and 10 mA. Energy Dispersive X-ray Spectroscopy (EDX) was employed to determine the elemental composition of the prepared material.

Fourier Transform Infrared Spectrometry (FTIR)

The chemical characteristics of the primer before and after modification with nano-chitosan loaded with calcium phosphate were analyzed using Fourier Transform Infra-Red spectroscopy (FTIR/ATR Alpha II, Platinum, Bruker Optic, Germany) at a wavelength range of 400-4000 cm^{-1}, 24 scans at 4 cm^{-1} resolution. The FTIR spectrum of unmodified primer was used as a reference for the changes detected [21,22].

Degree of Monomer Conversion (DC)

Using FTIR Spectroscopy, the DC assessment was comparable to that reported by Gutiérrez et al. [23], 5 specimens for each group were prepared by applying a drop of primer (10μL) on a celluloid strip fixed over a glass slide and gently pressed by another strip. Then the specimen was light cured at 1500W/cm^2 for 10s (5 seconds from each side), with consideration for a standard distance of 1 mm between the tip of the light unit and the sample. The upper celluloid strips were removed, and the cured specimen (4*6 mm in dimensions and thickness of approximately 0.1 mm), was carefully removed with a narrow surgical blade and stored for 24 hours in a dry dark container until analysis. After that the specimen was placed on the diamond of the metal circlip of a "Fourier-transform infrared spectroscope (FTIR)" equipped with attenuated total reflection, the spectrum was carried out in the absorbance mode with a wavelength range 400-4000 cm^{-1}, 24 scans at 4 cm^{-1} resolution. Non-cured drops of control and modified primer specimens were also subjected to FTIR spectroscopy [24].

The DC% was measured by a relative percentage basis (the tangent baseline and the two-frequency method) employing the C=C aliphatic bond stretching vibrations (analytical bond at 1638 cm^{-1}) and the C..C aromatic bond stretching vibrations (reference bond at 1608 cm^{-1}) which were not influenced by the setting reaction. The following Equation 1 was used to determine the DC:

$$\%DC = 100 \times 1 - \left(\frac{AP(\mathrm{C=C}) * AM(\mathrm{C-C})}{AP(\mathrm{C-C}) * AM(\mathrm{C=C})} \right) \quad (1)$$

where: A (C=C), A(C..C): the net peak absorbance areas of the set (P) and unset (M) material at the specific bands, respectively.

Shear bond strength (SBS)

The sample size was calculated using the following Formula 2:

$$N = \left[\left(4\sigma^2\right) \left(Z_\alpha + Z_\beta\right)^2 \right] \div E2 \quad (2)$$

where: N: The number of experimental samples; σ: The assumed standard deviation, it was =2.31 [25]; Zα =1.96 for a=0.05 (two-tailed), Zβ = 0.80 for the 80% power; E: The detectable difference between treatment means = 4.

The sample size estimation involved 10 teeth for each study group. In accordance with the above formula, the study samples consisted of 30 human premolar teeth, free of enamel cracks, filling, and caries which were extracted for orthodontic purposes. The teeth were cleaned from debris and stored in a 0.1% thymol solution to inhibit bacterial growth [26,27]. The roots of all teeth were embedded in blocks of acrylic resin for stability during testing with only the crown surfaces exposed. After polishing the buccal surfaces of the teeth with non-fluoridated pumice, they were rinsed with water and dried. For brackets bonding, (37%) phosphoric acid was

used to etch the teeth for (20) sec, rinsed for (10) sec, and air dried.

The unmodified and modified primer was then painted on the premolar buccal surfaces, and a gentle airflow was applied to disperse any excess primer. Orthodontic brackets (Stainless Steel Metallic Brackets, Standard Edgewise type, Dentaurum, Germany) were positioned with a Boone gauge approximately 4 mm from the tip of the buccal cusp [28] and pressed by a load of 200 g, monitored by computer software connected to the universal testing machine (Gester instrument Co, Fujian, PR China). after removing the excess adhesive, the brackets were cured from both the mesial and distal sides for 20 secs, using LED light curing device (1500 mW/cm^2), keeping a distance of 2 mm away from the bracket. The SBS test

was conducted using a universal testing machine [29-31]. A knife-edge chisel was positioned at the tooth-bracket interface (Figure 1) and the crosshead speed was set to 0.5mm/min. The results of the fracture force were electronically recorded in Newton and transformed into Megapascals by dividing the force by the surface area of the bracket base (10 mm^2).

Testing the wettability

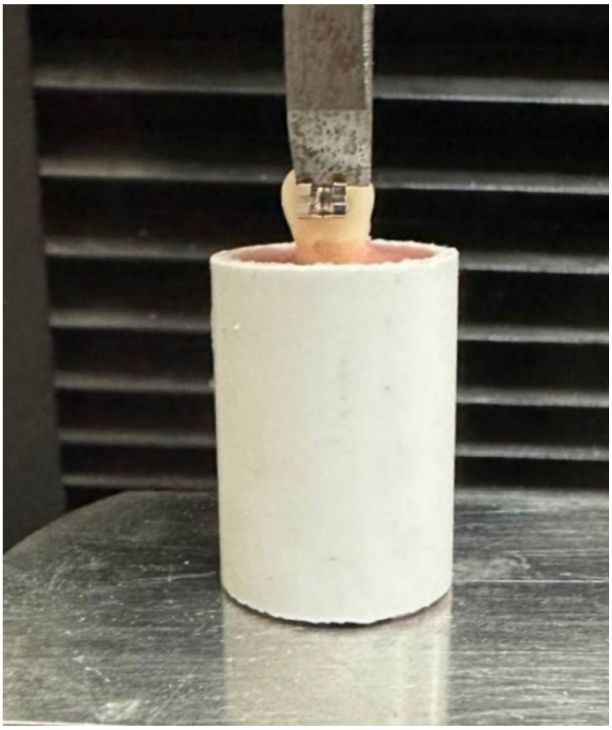

Figure 1 - Bracket under constant pressure during the shear bond strength testing.

Wettability was assessed by measuring the contact angle of the adhesive primer [32] by a sessile drop method at room temperature (25 ± 0.5 °C) using a contact angle goniometer a drop (5 μl) of each group (control primer, 5%, and 10% ChCPP) was dispensed using a micropipette onto a smooth, flat aluminum plate covered with polytetrafluoroethylene tape [33] The plate was then positioned on the sample table of a contact angle goniometer. This procedure was repeated five times for each group, and a total of 15 images were captured. The contact angles were measured using drop shape analysis in the Image J software program (Figure 2).

Disc diffusion method for antibacterial analysis: (Kirby-Bauer method)

Plastic molds (5 mm in diameter and 1 mm in thickness) were used to fabricate discs for the control, 5% ChCPP, and 10% ChCPP groups (total discs =15, n=5 for each group). The primer was poured into the molds and light-cured for 20 sec, the discs were removed from the molds and sterilized with 70% alcohol for 30 minutes at room temperature and placed inside a sterilization pouch. A sterilization check was performed by incubating one disc in broth media for 24 hours, showing no growth.

The antibacterial activity of the modified adhesive discs was tested against *Streptococcus mutans* (gram positive) and *Lactobacillus acidophilus* (gram negative) bacteria.

Brain heart infusion (BHI) broth was used to culture *S. mutans* and *Lactobacillus* individually; with turbidity equal to 0.5 standard (about 150 million cells per mL), the tubes were incubated for 18 hours at 37 °C.

The Mueller-Hinton Agar plate was smeared with bacterial culture and allowed to dry for about (5) min. A sterilized forceps was used to press the discs onto the agar surface [34]. Plates incubations were done in anaerobic conditions at 37 °C for 48 hours. The diameter of the bacterial inhibition zone surrounding the discs was measured in millimeters using Image J software.

An inter-examiner calibration was carried out by repeating the measurements of all groups by a second experienced operator (both of them were blinded to the experimental groups), The results revealed no significant differences between the two sets of readings.

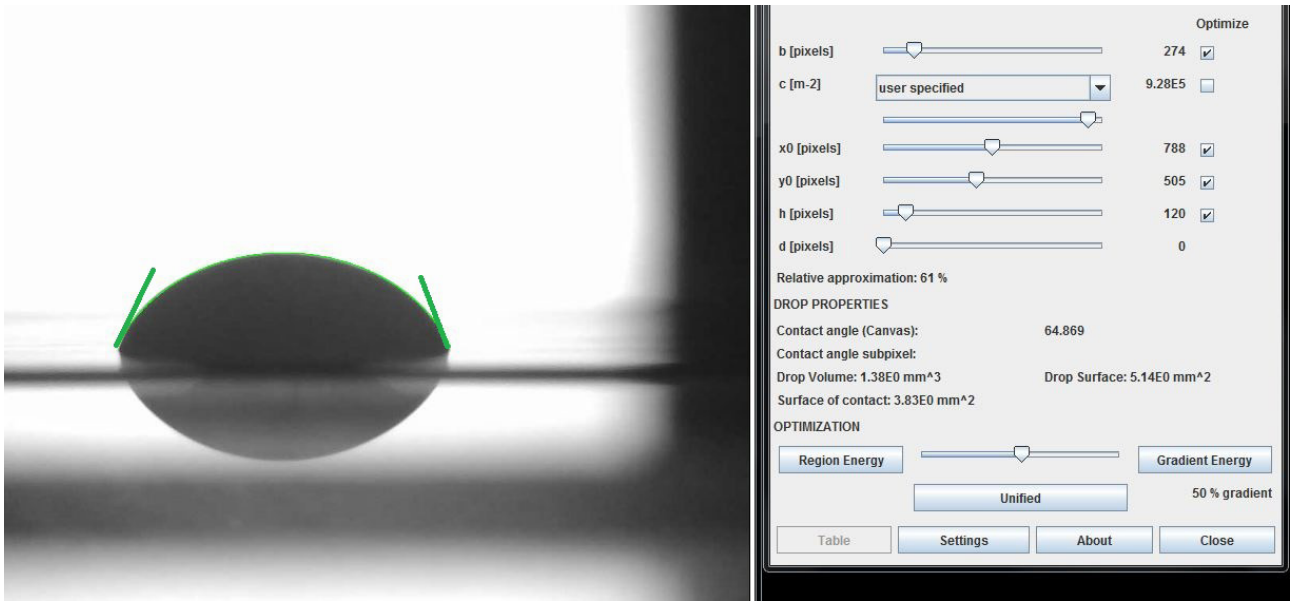

Figure 2 - Contact angle measurement of droplet by Image J software.

Five Petri dishes were used for each type of bacteria with each dish containing 3 discs: control, 5% ChCPP, and 10% ChCPP [35].

FESEM-EDX analysis of remineralization

Before assessing the remineralization effect of modified orthodontic primer, a demineralization process was conducted to eliminate false positive results. The demineralizing solution contained (2.2) mmol/L NaH_2PO_4, (2.2) mmol/L $CaCl_2$, and (50) mmol/L acetic acid, with NaOH added dropwise to adjust pH to 4.5 [36]. Fifteen maxillary premolar crowns of all groups (n=5) were painted with an acid-resistant varnish, leaving a window of enamel about 3 × 4 mm in the middle third of the buccal surface exposed to the acid attack, while the rest of the crown was protected by the varnish.

Each group was immersed in 40 mL of acidified buffered demineralizing solution at room temperature for 96 hours to develop initial artificial carious lesions. After removal from the demineralization solution, the specimens were washed and dried. The exposed enamel window on the demineralized specimen was then etched and bonded with control primer, 5% ChCPP, and 10% ChCPP. Each group was placed in a separate container with 40 mL artificial saliva for four months. Artificial saliva composition included: (0.4g/L) KCl, (0.4g/L) NaCl, (0.906 g/L) $CaCL_2.2H_2O$, (0.906 g/L) $NaH_2PO_4.2H_2O$, (0.005 g/L) $Na_2S.9H_2O$ and (1 g/L) Urea, dissolved in 1000 mL of distilled water [37].

For FESEM-EDX analysis, the crowns were separated from the roots using a low-speed water-cooled diamond cut-off disc, followed by a longitudinal section at the buccolingual direction in the mid of the occlusal surface of the premolars. The cut surfaces were stored in distilled water until measurements.

All specimens were thoroughly dried and gold-coated to prepare the surface suitable for examination by the FESEM.

The EDX analysis unit attached to the FESEM apparatus was used to measure elemental precipitation (calcium and phosphate weight %). The cut surfaces of the teeth were examined carefully at a depth of 100 μm from the bonding surface to obtain representative photographs and measurements.

RESULTS

Characterization of nano-chitosan/calcium phosphate by FESEM-EDX

The FESEM image (Figure 3A) of the prepared chitosan/ calcium phosphate shows calcium phosphate particles as pale spots, forming clusters within the chitosan matrix. In Figure 3B a homogeneous distribution of the calcium phosphate particles in the chitosan matrix is observed with a nano-size scale range of 30-60nm.

The homogenous distribution and cluster formation of the prepared solution indicates a

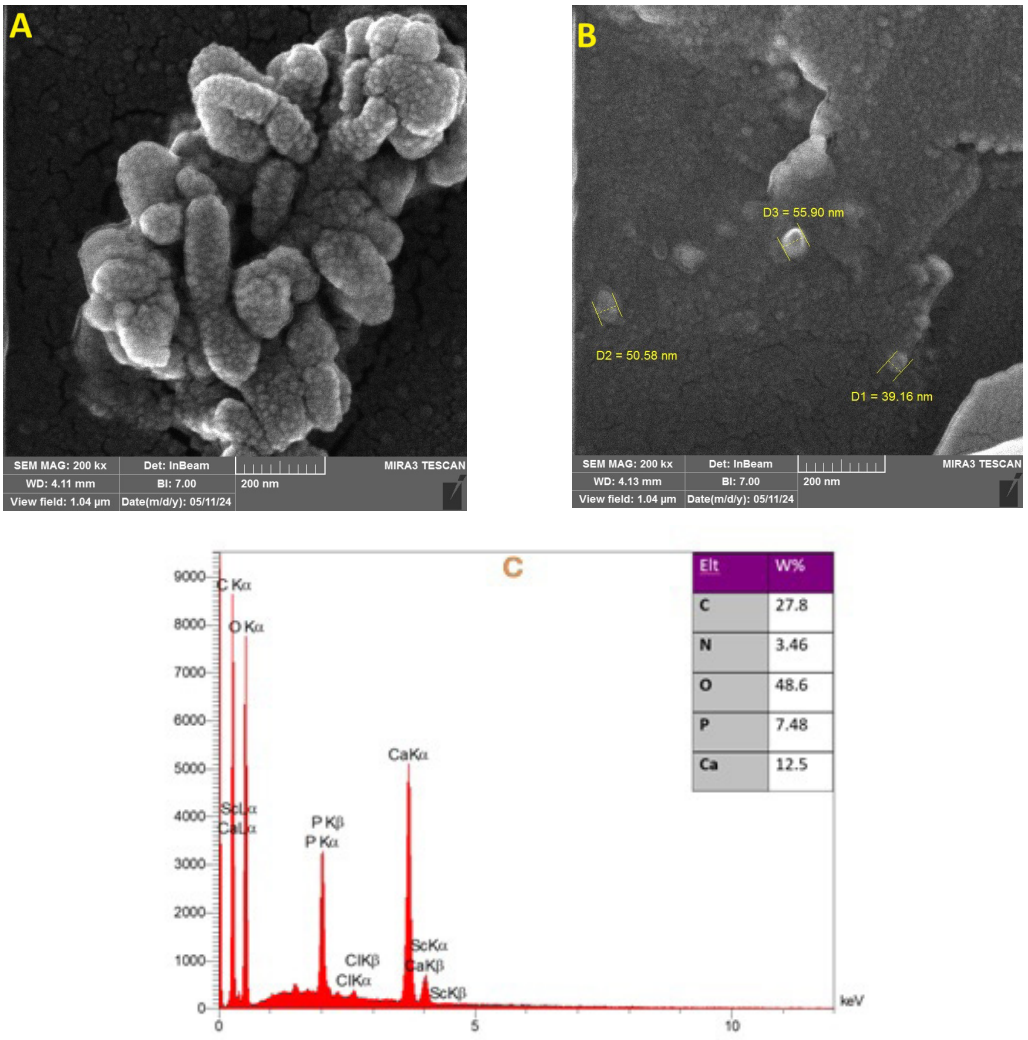

Figure 3 - (A) FESEM image of nano-chitosan loaded with calcium phosphate at 200 kx magnification showing a cluster formation of calcium phosphate within chitosan matrix; (B) Size of calcium phosphate particles; (C) EDX spectrum with elements percentage in weight of the prepared solution.

successful loading of the calcium phosphate in to the chitosan solution.

The EDX of chitosan/ calcium phosphate sample represented a higher proportion of Carbon (C) and Oxygen(O) with smaller percentage of nitrogen (N), calcium (Ca), and phosphate (P) (Figure 3C).

FTIR Characterization of modified primer by nano-chitosan loaded with calcium phosphate:

FTIR spectra of all groups are shown in Figures 4A, B and C indicating that no chemical reaction occurred between the primer and the calcium phosphate-loaded chitosan at 5% and 10%. This is evidenced by the absence of additional new bands or disappearing bands in the spectra.

Chitosan displays a distinct peak at 3436 cm^{-1} belongs to the hydroxyl stretch(O-H), and a peak at 1636 belongs to the (C = O) stretch of the amide I band.

The FTIR spectrum of the primer displays distinct peaks at 3436 cm^{-1}, 2959, 1714 cm^{-1}, and 1636 cm^{-1}, corresponding to hydroxyl(O-H), aliphatic(C-H), carbonyl (C=O), and alkene (C=C) stretching, respectively. these peaks overlap with those of chitosan indicating that no additional peaks are present between the FTIR spectra of the unmodified and modified primer.

Shear bond strength and degree of monomer conversion

The 10% ChCPP group exhibited the greatest significant mean value for both SBS and DC, followed by the 5% ChCPP group. The control group had the lowest mean values. No significant differences in SBS and DC were observed between 5% and 10% ChCPP groups as shown in Table II.

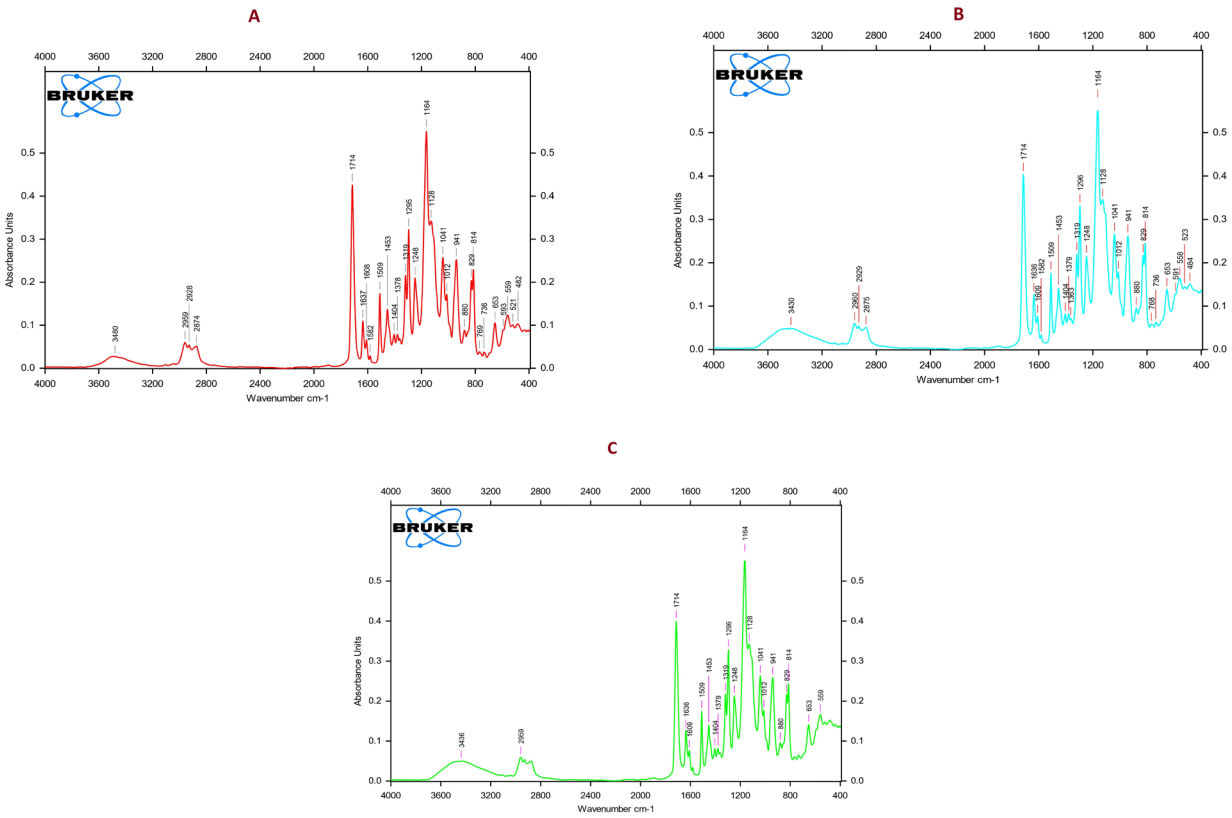

Figure 4 - FTIR spectra of (A) control; (B) 5% ChCPP; (C) 10%.

Wettability and contact angle measurement

Table III shows that the control group had a higher mean value of contact angle measurement compared to the modified groups, although the differences were not statistically significant. This indicates that 5% and 10% ChCPP groups improved the wettability of the orthodontic resin.

Antibacterial Action on *S. mutans* and *Lactobacillus acidophilus*

The antimicrobial test results displayed that both the 5% and 10% ChCPP experimental discs exhibited antibacterial activity against *S. mutans* and *Lactobacillus* as indicated by the clear inhibition zones around the discs on the agar plates, as shown in Figure 5A and B. In contrast, no clear zone was observed around the discs in the control group indicating no antibacterial effect. The antibacterial effect significantly increased from 5% to 10% ChCPP (Table IV).

FESEM-EDX analysis of remineralized enamel

The morphology of hydroxy appetite crystals, inter-rod spaces, and mineral depositions on the surface of treated groups is demonstrated in the FESEM images (Figure 6 from A1 to C2).

After 4 months of remineralization with ChCPP, grain-like new materials modified the nanocrystalline structures of the enamel (prisms and inter-prismatic areas). Filling the acid-demineralized lesions with enamel-like structures. These changes suggest that non-classical crystallization mechanisms likely contributed to the formation of the new structures.

Additionally, the treated groups displayed mineral deposition and the formation of hydroxyapatite layers on the demineralized enamel beyond the adhesive layer (Figure 6: B1, B2, C1, C2).

The 10% ChCPP group showed a greater reduction in inter-rod spaces and more mineral deposition than 5% ChCPP group, while no such changes were observed in the control group

In the EDX analysis (Figure 6: A3, B3, C3), the primary elements identified in the enamel were oxygen (O), calcium (Ca), and phosphorus (P) with small amounts of carbon (C), magnesium (Mg), sodium (Na), and chlorine (Cl). Table V summarizes the means and standard deviation of the weight percentages of mineral concentrations.

Table II - Descriptive statistics and multiple comparisons Post-hoc Tukey test of shear bond strength and degree of conversion of the control, 5% ChCPP, 10% ChCPP, significant difference at (P ≤ 0.05)

	Shear Bond Strength					Degree of Conversion				
Groups	n	Mean (MPa)	SD	p - value	Post-hoc test*	N	Mean (%)	SD	p - value	Post-hoc test*
Control	10	15.2	2.4		A	5	60.26	1.25		A
5% ChCPP	10	18.52	2.2	0.01	B	5	67	1.45	0.000	B
10% ChCPP	10	20.85	3.7		B	5	68.2	1.42		B

ChCPP: Chitosan/Calcium Phosphate Primer; SD: Standard deviation. *Different letters mean significant difference (p ≤ 0.05).

Table III - Descriptive statistics and multiple comparisons Post-hoc Tukey test of contact angle measurements of the control, 5% ChCPP, 10% ChCPP, significant difference at (P ≤ 0.05)

Groups	N	Mean	SD	Min.	Max.	p - value	Post-hoc test*
Control	5	68.1	3.1	65	72.3		A
5% ChCPP	5	63.4	3.5	58	68.4	0.06	A
10% ChPP	5	63.6	1.865	60.5	65.3		A

ChCPP: Chitosan/Calcium Phosphate Primer; SD: Standard deviation. *Different letters mean significant difference (p ≤ 0.05).

Table IV - Descriptive statistics and multiple comparisons Post-hoc Tukey test of *S. mutans* and *Lactobacillus growth* inhibition of the control, 5% ChCPP, 10% ChCPP, significant difference at (P ≤ 0.05).

	Streptococcus mutans					*Lactobacillus*				
Groups	n	Mean (mm)	SD	p- value	Post-hoc test*	n	Mean (mm)	SD	p- value	Post-hoc test*
Control	5	0	0		A	5	0	0		A
5% ChCPP	5	7.42	0.88	0.000	B	5	5.64	.75	0.000	B
10% ChCPP	5	12.26	0.93		C	5	11.72	.74		C

ChCPP: Chitosan/Calcium Phosphate Primer; SD: Standard deviation. *Different letters mean significant difference (p ≤ 0.05).

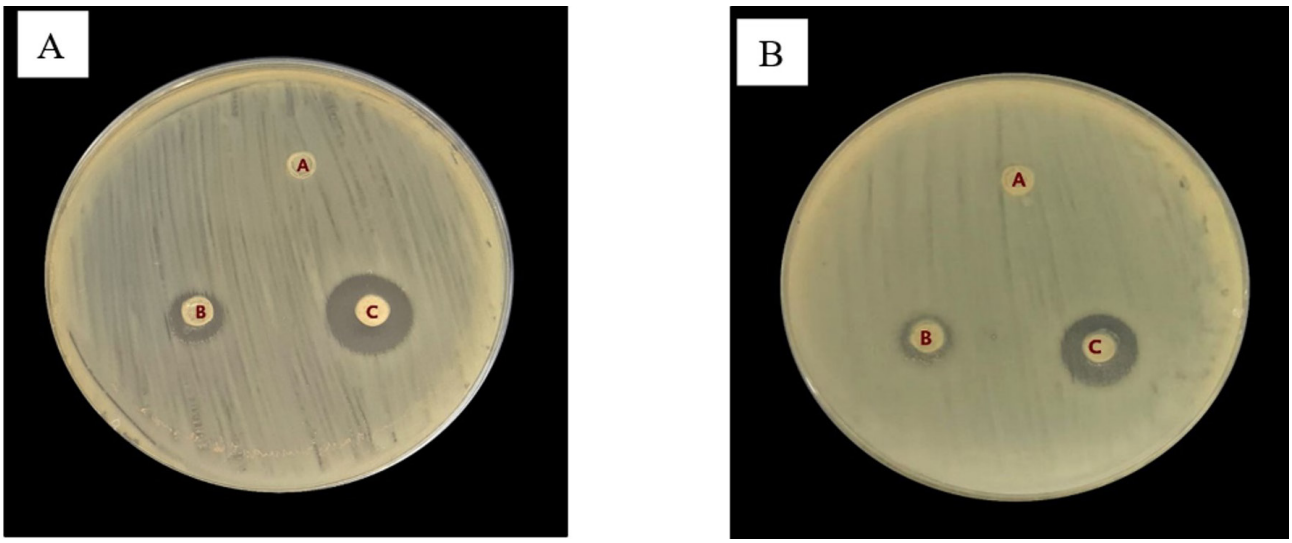

Figure 5 - Bacterial inhibition zone against: (A) *S. mutans* and (B) *Lactobacillus*. Disc A for control group, Disc B for 5% ChCPP and Disc C for 10% ChCPP.

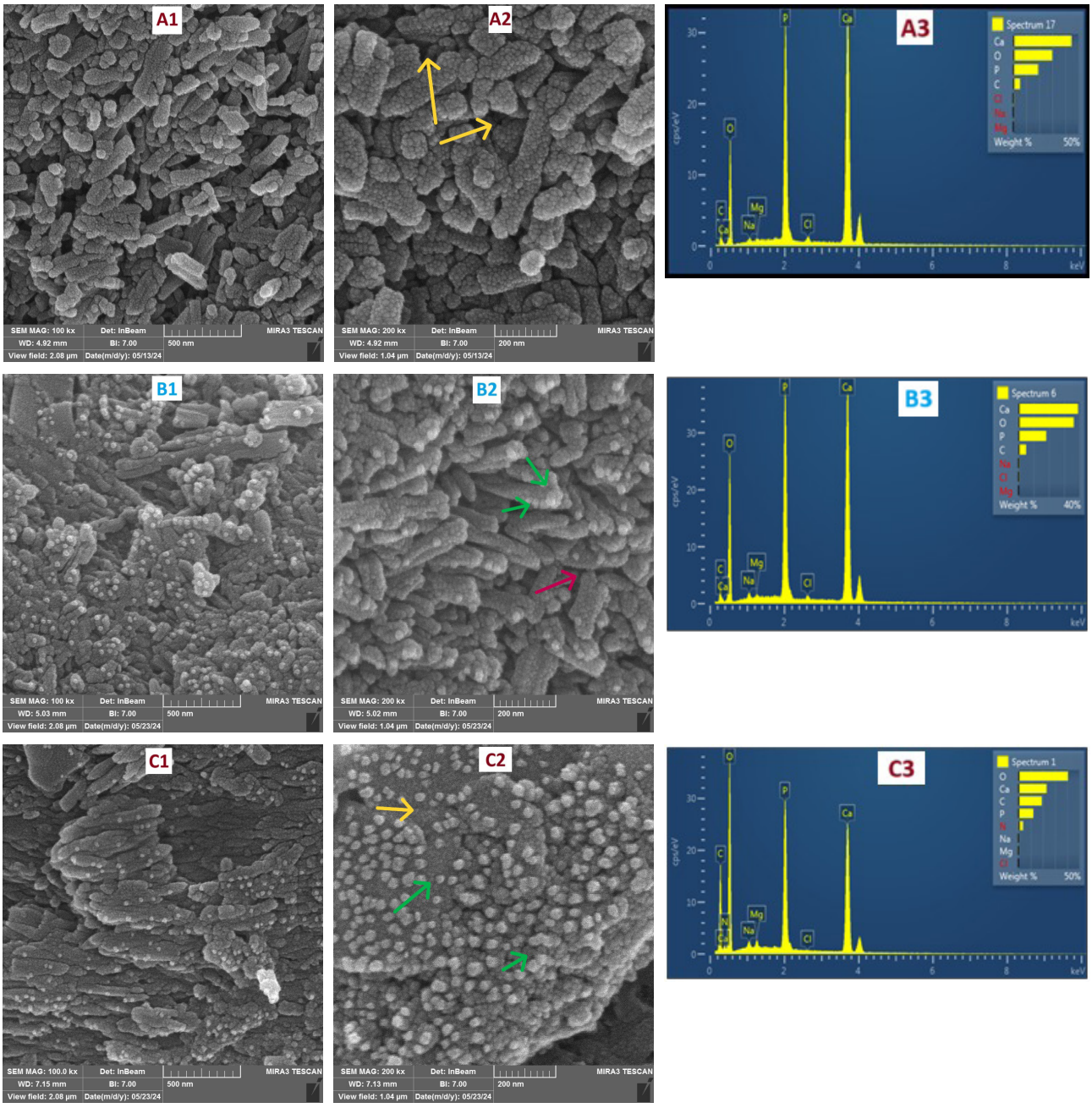

Figure 6 - SEM images of the teeth cross section after remineralization at 100kx and 200kx magnifications: A1, A2 for the control group; B1, B2 for 5%ChCPP, C1, C2 for 10% ChCPP. Yellow arrow showed the inter-rods spaces of control group. Red arrows showed decreased spaces. The green arrows represent the calcium phosphate precipitation. A3, B3, and C3 showed the EDX analysis for each group.

Table V - Descriptive statistics and multiple comparisons Post-hoc Tukey test of EDX of calcium wt %, phosphate wt % and Ca/P ratio of the control, 5% ChCPP, 10% ChCPP, significant difference at (P ≤ 0.05)

Elements	Control (n=5)	5% ChCPP (n=5)	10% ChCPP (n=5)	p-value	Tukey test* control	Tukey test* 5% ChCPP	Tukey test* 10% ChCPP
Ca wt % (mean ± SD)	26.42 ± 6.46	32.92 ± 3.08	36.04 ± 3.21	0.017	A	AB	B
P wt % (mean ± SD)	13.98 ± 2.18	15.83 ± 1.37	17.30 ± 1.9	0.046	A	AB	B
Ca/P (mean ± SD)	1.75 ± 0.19	2.07 ± 0.79	2.08 ± 1.57	0.007	A	B	B

ChCPP: Chitosan/Calcium Phosphate Primer; SD: Standard deviation. *Different letters mean significant difference (p ≤ 0.05).

ANOVA analysis revealed significant differences in calcium and phosphorus concentration across the three groups following remineralization ($p < 0.05$) (Table V). Both 5% and 10% ChCPP groups had higher mean calcium and phosphorus levels than the control group.

The10% ChCPP showed a significant difference from the control group, while the 5% ChCPP group did not show significant differences from both the control and 10% ChCPP groups.

On comparing the Ca/P ratio, ANOVA showed significant differences in the Ca/P ratio among the three groups after remineralization ($p < 0.05$) (Table V). The Ca/P ratios of the 5% and 10% ChCPP groups were significantly higher than those of the control group. Additionally, the 10% ChCPP group had a nonsignificant higher mean value of Ca/P ratio compared to 5% ChCPP group.

DISCUSSION

In this study, the addition of nano-chitosan loaded with tricalcium phosphate to the orthodontic adhesive showed antimicrobial activity against dental caries-producing bacteria and showed clear mineral precipitation indicating its potential for remineralizing of the demineralized enamel. Additionally, it enhanced the physical and chemical properties of the primer. Therefore, the null hypothesis was rejected.

The modification of the orthodontic adhesive primer with antibacterial and remineralizing agents requires careful testing of bond strength because the treatment is negatively affected by both high and low SBS. Excessive SBS values above 60 MPa can lead to enamel fractures during brackets debonding, while lower SBS values below 6-8 MPa may result in brackets debonding and prolong orthodontic treatment [38,39]. The current study showed a significant increase in SBS by incorporating 5% and 10% nano-chitosan loaded with calcium phosphate into orthodontic primer within the acceptable range compared to the control group. This enhancement can be attributed to the nanoparticles acting as stress-absorbing elements, which provide structural reinforcement and reduce the concentration of interfacial stress [40]. These results are comparable to other studies [40,41] that found the addition of chitosan to orthodontic primer increased the SBS. However, other researches [39,42], using different molecular weights and concentrations of chitosan nanoparticles in orthodontic adhesives found no significant differences in SBS, suggesting that the impact of chitosan addition on the mechanical properties may vary based on formulation.

Degree of conversion (DC) was assessed in this study to evaluate the proportion of monomers that react to form polymers or the proportion of C=C double bonds that convert into C-C single bonds [43]. The DC% plays a crucial role in determining the physical properties of cross-linked polymers. A high DC typically correlates with improved mechanical properties, less susceptibility to degradation, and lower levels of residual monomers in the organic matrix leading to reduced monomer leaching and cytotoxicity [44]. Notably, residual monomers can still be detected after prolonged immersion of up to 52 weeks [45].

Our study showed a significant increase in the degree of monomer conversion and improved adhesive polymerization in both 5% and 10% ChCPP groups compared to the control group. This result aligns with the findings of Tanaka et al. [46], who observed an increase in DC in dental composites with the addition of chitosan-loaded dibasic calcium phosphate fillers. Similarly, Chanachai et al. [47] modified orthodontic adhesives with calcium phosphate and nisin, achieving a comparable degree of conversion to commercial adhesives, although with decreased mechanical properties. In contrast, Mahapoka et al. [48] reported a non-significant decrease in the DC of Chitosan whiskers incorporated into dental resin compared to the control group. Moreover, Machado et al. [44] found that the adding 2 or 5 wt.% chitosan or triclosan-loaded chitosan showed non-significant differences in DC from the control group.

The discrepancies between these findings and our results may be attributed to variations in methodology. Both Mahapoka's and Machado's studies used solid chitosan, which may have hindered light transmission through the adhesive film, thereby slowing down the photopolymerization process [49]; In contrast, our study used chitosan loaded with calcium phosphate in liquid form, which did not affect the translucency of the primer and thus did not interfere with the polymerization process.

The mean DC values across all groups in our study were within the clinically acceptable range of 55% to 75%, as suggested by Kauppi and Combe [50]. The improvement in monomer conversion observed in our study may be due to the photooxidative degradation of chitosan during light curing, which leads to polymer chain breakage. This process generates free

radicals, reducing the molecular weight and viscosity of the polymer, ultimately enhancing the polymerization process and increasing DC [51].

Regarding the contact angle measurements of the primer, the angle is formed at a three-phase junction where solid, liquid, and gas intersect [52]. When the CA is less than 90°, it indicates that the liquid (primer) wets the etched enamel surface, promoting better adhesion. Conversely, if the CA is greater than 90°, it suggests non-wetting of the substrate, which may negatively affect adhesion. Complete wetting is achieved when the contact angle is zero degrees, signifying ideal adhesion conditions [32].

The bonding efficiency of the bracket base is primarily influenced by the ability of the primer to wet and adapt to the etched enamel surface. The wettability of a liquid primer is closely related to its contact angle (CA), with an inverse relationship between them, meaning better wettability is associated with a lower CA [32].

In this study, the CA of the modified adhesive with 5% and 10% chitosan/calcium phosphate was lower compared to the control group, although no statistically significant differences were found between the modified groups.

The reduction in CA might be attributed to the dilution effect caused by the incorporation of the chitosan solution, which likely led to a decrease in the primer's viscosity, enhancing its ability to spread across the enamel surface. Improved wettability at a lower contact angle and contributes to better adaptation of the primer to the surface, enhancing the bonding strength.

These findings align with the study by Katyal et al. [41], which also reported a decrease in CA for the nano-chitosan modified orthodontic primer compared to non-modified primer. This suggests that the incorporation of chitosan in primer formulations can improve surface wetting and potentially improve bond strength without negatively affecting the adhesive's performance.

A study of Niu et al. [53] reported decreased values of CA by increasing the concentration of phosphorylated chitosan loaded with amorphous calcium phosphate (Pchi/ACP) added into a composite resin. This reduction in CA was attributed to the hydrophilic components of HEMA (hydroxyethyl methacrylate) and Pchi. which promote better surface wetting and interaction with the substrate [53].

Chitosan also possesses notable antibacterial activity [54,55], as it acts as an adhesive agent that binds to the negatively charged cell wall. This interaction disrupts the bacterial cell's functions by interfering with DNA replication leading to cell destruction [41].

Two types of bacteria were investigated in this study: *Streptococcus mutans* and *Lactobacillus acidophilus*. The results showed that 5% and 10% ChCPP groups had antibacterial effects against both *S. mutans* and *Lactobacillus acidophilus* with a significant increase in its activity by increasing the concentration, these results agree with Yao et al. [56] who concluded that 20 mg/mL carboxymethyl chitosan (CMC) modified adhesive system, revealed antibacterial action against *S. mutans*. Kikuchi et al. [57] showed that reduction of biofilm formation can be achieved by 16 hours crosslinking of chitosan particles loaded with dibasic calcium phosphate (DCPA). Another study by Harini et al. [58] claimed that a maximum inhibition zone against *S. mutans* was achieved by chitosan-based dental varnish. Also, Mirhashemi et al. [59] suggested that orthodontic composite modified by chitosan had antibacterial activity against *S. sangius, S. mutans*, and *Lactobacillus acidophilus*.

Overall, the data supports the use of chitosan and its derivatives in enhancing the antibacterial properties of orthodontic materials, potentially improving oral health outcomes during orthodontic treatment [60].

The FESEM images in Figure 6 showed mineral precipitation indicating that both 5 and 10% ChCPP groups were capable of remineralizing the demineralized enamel and this finding aligns with the study by Simeonov et al. [61], which reported that chitosan/calcium phosphate microgels effectively remineralize demineralized enamel surfaces by promoting calcium phosphate nucleation and development. Chitosan served as a scaffold for calcium phosphate deposition, facilitating the in-situ formation of amorphous to weakly crystalline hydroxyapatite (HAP) crystals.

Furthermore, Song et al. [62] loaded ACP by carboxy-methyl chitosan/lysozyme nano gel and evaluated remineralization ability by forming a prismatic enamel-like structure over the demineralized surface. Wahied et al. [63] reported that nanohydroxyapatite and nano β-TCP loaded by nano-chitosan acted as active remineralizing agents with promising results.

In this study, EDX analysis revealed that greater calcium and phosphate were precipitated in the area beyond the adhesive layer. These findings are consistent with the study by Neu et al. [53], which suggested that incorporating phosphorylated chitosan/ amorphous calcium phosphate (Pchi/ACP) into composite resin led to higher mineral deposits of calcium and phosphorus weight fractions on dentin surfaces of treated dentin slabs.

It has been found from previous studies that the Ca/P ratio is a key element in the nucleation of calcium phosphate [64]. In our study, the Ca/P increased in the 5% and 10% ChCPP groups compared to the control group. This observation aligns with the research conducted by Paik et al. [65] who added a calcium phosphate ion cluster solution to demineralized enamel and reported enhancements in the Ca/P ratio and remineralization of early tooth lesions.

The advantages of chitosan loaded with calcium phosphate in enamel remineralization over calcium phosphate alone can be explained by the fact that chitosan acts as a template for molecular interaction with the minerals to control HAP growth in the mineralization process. In acidic conditions, the protonation of the amino groups in the chitosan molecule results in a positive charge. The positively charged chitosan calcium phosphates attract to the negatively charged enamel surfaces and promote the adhesion between them, furthermore, chitosan functions as a reservoir for Ca and P ions, giving the demineralized enamel with the mineral ions essential for the biomimetic mineralization [63].

CONCLUSIONS

Under the limitations of this study, the following conclusions can be drawn based on the results and discussion:

1. *Improved Adhesive Properties*: The modified orthodontic primer containing 5% and 10% chitosan/calcium phosphate (ChCPP) demonstrated significant improvements in shear bond strength (SBS), contact angle (CA), and degree of conversion (DC);
2. *Antibacterial Activity*: Both the 5% and 10% ChCPP formulations exhibited effective antibacterial properties against *Streptococcus mutans* and *Lactobacillus acidophilus*, suggesting their potential for caries prevention;
3. *Remineralization of Enamel*: The ChCPP formulations were shown to promote remineralization of demineralized enamel after four months of immersion in artificial saliva, resulting in mineral deposition and an increased calcium-to-phosphate (Ca/P) ratio compared to the control group;
4. *Enhanced Performance of 10% ChCPP:* The 10% ChCPP group displayed superior improvements across all adhesive properties compared to the 5% ChCPP group, making it a more promising candidate for orthodontic adhesive applications.

These findings support the potential of incorporating ChCPP into orthodontic adhesives to enhance their performance and contribute to dental health.

Limitation

1. This in vitro study was conducted under controlled laboratory conditions, which may not accurately replicate the complex oral environment, including variations in saliva composition, oral hygiene practices, and dietary factors.
2. The remineralization assessment was conducted over a fixed period (4 months). Longer-term studies may provide a more comprehensive understanding of the durability and effectiveness of the modified adhesives.
3. Antibacterial efficacy was evaluated against specific strains (*S. mutans* and *Lactobacillus acidophilus*). Future studies could assess the effectiveness against a broader range of bacteria, including oral biofilm and other cariogenic pathogens.

Suggestions

- Evaluation of the remineralizing properties of chitosan loaded with calcium phosphate in vivo conditions;
- Assess the calcium and phosphate ion release;
- The effects of adding chitosan/ calcium phosphate to other dental products like toothpaste, varnishes, and other preventive measures.

Acknowledgements

The authors wish to express their gratitude to College of Dentistry, University of Mosul for providing all necessary assistance that helped them to conduct this research.

Author's Contributions

LRAB: Methodology, Investigation, Resources, Data Curation, Writing – Original Draft Preparation, Writing – Review & Editing, Visualization. ARAK: Supervision. FHJ: Supervision.

Conflict of Interest

No conflicts of interest declared concerning the publication of this article.

Funding

The authors declare that no financial support was received.

Regulatory Statement

The present study did not include the use of hazardous materials, or any procedures that could potentially harm the environment. It was conducted in accordance with all the provisions of University of Mosul Ethical Committee Agency. The approval code for this study is: UoM.Dent. 23/24.

REFERENCES

1. Araújo DFG, Lucena FS, Freitas MCCA, Nunes LV, Velo MMAC, Magalhães AC, et al. Effect of enamel pretreatment on the fluoride remineralization of artificial white spot lesions. Braz Dent Sci. 2018;21(3):328-34. http://doi.org/10.14295/bds.2018.v21i3.1585.
2. Al-Banaa LR, Alsoufy SS, Al-Khatib AR. Factors contributing to microleakage in orthodontics: a review of literature. Al-Rafidain Dent J. 2022;22(2):376-88. http://doi.org/10.33899/rdenj.2022.131409.1136.
3. Nyvad B, Machiulskiene V, Baelum V. Reliability of a new caries diagnostic system differentiating between active and inactive caries lesions. Caries Res. 1999;33(4):252-60. http://doi.org/10.1159/000016526. PMid:10343087.
4. Ünal S, Bakir S, Bakir EP. Evaluation of the antibacterial effects of four different adhesives against three bacterial species in two time periods: an in vitro comparative study. J. Adv. Oral Res. 2022;13(1):120-6. http://doi.org/10.1177/23202068221084452.
5. Ahirwar SS, Gupta MK, Snehi SK. Dental caries and lactobacillus: role and ecology in the oral cavity. Int J Pharm Sci Res. 2019;11:4818-29.
6. Arifa MK, Ephraim R, Rajamani T. Recent advances in dental hard tissue remineralization: a review of literature. Int J Clin Pediatr Dent. 2019;12(2):139-44. http://doi.org/10.5005/jp-journals-10005-1603. PMid:31571787.
7. Dorozhkin SV. Calcium Orthophosphates (CaPo) and Dentistry. Bioceram. Dev. Appl. 2016;06(2). http://doi.org/10.4172/2090-5025.1000096.
8. Khan AS, Syed MR. A review of bioceramics-based dental restorative materials. Dent Mater J. 2019;38(2):163-76. http://doi.org/10.4012/dmj.2018-039. PMid:30381635.
9. Nimbeni SB, Nimbeni BS, Divakar DD. Role of chitosan in remineralization of enamel and dentin: a systematic review. Int J Clin Pediatr Dent. 2021;14(4):562-8. http://doi.org/10.5005/jp-journals-10005-1971. PMid:34824515.
10. Abd El-Hack ME, El-Saadony MT, Shafi ME, Zabermawi NM, Arif M, Batiha GE, et al. Antimicrobial and antioxidant properties of chitosan and its derivatives and their applications: a review. Int J Biol Macromol. 2020;164:2726-44. http://doi.org/10.1016/j.ijbiomac.2020.08.153. PMid:32841671.
11. Elsaka SE. Antibacterial activity and adhesive properties of a chitosan-containing dental adhesive. Quintessence Int. 2012;43(7):603-13. PMid:22670256.
12. Husain S, Al-Samadani KH, Najeeb S, Zafar MS, Khurshid Z, Zohaib S, et al. Chitosan biomaterials for current and potential dental applications. Materials. 2017;10(6):602. http://doi.org/10.3390/ma10060602. PMid:28772963.
13. Goy RC, Morais STB, Assis OBG. Evaluation of the antimicrobial activity of chitosan and its quaternized derivative on *E. coli* and *S. aureus* growth. Rev Bras Farmacogn. 2016;26(1):122-7. http://doi.org/10.1016/j.bjp.2015.09.010.
14. Santoso T, Djauharie NK, Ahdi W, Latief FDE, Suprastiwi E. Carboxymethyl chitosan/amorphous calcium phosphate and dentin remineralization. J Int Dent Med Res. 2019;12:84-7.
15. He L-H, Yao L, Xue R, Sun J, Song R. In-situ mineralization of chitosan/calcium phosphate composite and the effect of solvent on the structure. Front Mater Sci. 2011;5(3):282-92. http://doi.org/10.1007/s11706-011-0140-6.
16. Zaharia A, Mușat V, Anghel EM, Atkinson I, Mocioiu O-C, Bușilă M, et al. Biomimetic chitosan-hydroxyapatite hybrid biocoatings for enamel remineralization. Ceram Int. 2017;43(14):11390-402. http://doi.org/10.1016/j.ceramint.2017.05.346.
17. Xiao Z, Que K, Wang H, An R, Chen Z, Qiu Z, et al. Rapid biomimetic remineralization of the demineralized enamel surface using nano-particles of amorphous calcium phosphate guided by chimaeric peptides. Dent Mater. 2017;33(11):1217-28. http://doi.org/10.1016/j.dental.2017.07.015. PMid:28774431.
18. Wang X, Shi J, Li Z, Zhang S, Wu H, Jiang Z, et al. Facile one-pot preparation of chitosan/calcium pyrophosphate hybrid microflowers. ACS Appl Mater Interfaces. 2014;6(16):14522-32. http://doi.org/10.1021/am503787h. PMid:25065382.
19. Hameed AR, Majdoub H, Jabrail FH. Effects of surface morphology and type of cross-linking of chitosan-pectin microspheres on their degree of swelling and favipiravir release behavior. Polymers. 2023;15(15):3173. http://doi.org/10.3390/polym15153173. PMid:37571067.
20. Nader A, Sodagar A, Akhavan A, Pourhajibagher M, Bahador A. Antibacterial effects of orthodontic primer harboring chitosan nanoparticles against the multispecies biofilm of cariogenic bacteria in a rat model. Folia Med. 2020;62(4):817-24. http://doi.org/10.3897/folmed.62.e50200. PMid:33415933.
21. Ahmed MK, Alsaleem NR, AlSamak S. The effect of vanillin nanoparticles on antimicrobial and mechanical properties of an orthodontic adhesive. J Orthod Sci. 2023;12(1):46. http://doi.org/10.4103/jos.jos_124_22. PMid:37881677.
22. Saxena K, Ann CM, Azwar MABM, Banavar SR, Matinlinna J, Peters OA, et al. Effect of strontium fluoride on mechanical and remineralization properties of enamel: an in-vitro study on a modified orthodontic adhesive. Dent Mater. 2024;40(5):811-23. http://doi.org/10.1016/j.dental.2024.02.010. PMid:38490919.

23. Gutiérrez MF, Malaquias P, Matos TP, Szesz A, Souza S, Bermudez J, et al. Mechanical and microbiological properties and drug release modeling of an etch-and-rinse adhesive containing copper nanoparticles. Dent Mater. 2017;33(3):309-20. http://doi.org/10.1016/j.dental.2016.12.011. PMid:28094025.

24. Topbasi NM, Benkli YA. Evaluation of the bond strength of orthodontic brackets and the degree of polymerisation and microhardness of an orthodontic adhesive using polyvawe light curing unit and varying light densities. Braz Dent Sci. 2020;23(4):9. http://doi.org/10.14295/bds.2020.v23i4.2044.

25. Abdulhaddi A, Al Qassar SSS, Mohammed AM. Assessment of the mechanical properties and antimicrobial efficiency of orthodontic adhesive modified with *Salvadora Persica* oil. Ro J Stomatol. 2024;70(2):153-9. http://doi.org/10.37897/RJS.2024.2.14.

26. Al-Banaa LR. Evaluation of microleakage for three types of light cure orthodontic band cement. J Oral Biol Craniofac Res. 2022;12(3):352-7. http://doi.org/10.1016/j.jobcr.2022.04.004. PMid:35514676.

27. Monteiro JB, Abreu RT, Salgado L, Paradella TC, Salgado IO, Cilli R. Effect of shear bond strength of metallic orthodontic brackets bonded with and without dental adhesive. Braz Dent Sci. 2018;21(4):395-402. http://doi.org/10.14295/bds.2018.v21i4.1597.

28. AlSamak S, Alsaleem NR, Ahmed MK. Evaluation of the shear bond strength and adhesive remnant index of color change, fluorescent, and conventional orthodontic adhesives: an in vitro study. Int Orthod. 2023;21(1):100712. http://doi.org/10.1016/j.ortho.2022.100712. PMid:36493626.

29. Abutayyem H. In-vitro investigation of the shear bond strength of different orthodontic adhesives to enamel. J Pharm Bioallied Sci. 2024;16(Suppl 3):S2473-5. http://doi.org/10.4103/jpbs.jpbs_323_24. PMid:39346208.

30. Althagafi NM. Impact of fluoride-releasing orthodontic adhesives on the shear bond strength of orthodontic brackets to eroded enamel following different surface treatment protocols. J Orthod Sci. 2022;11(1):3. http://doi.org/10.4103/jos.jos_139_21. PMid:35282290.

31. Araújo IJS, Zanini MM, Favarão J, Rontani RMP, Correr AB, Sinhoreti MAC. Bond strength of different orthodontic brackets produced with different materials and fabrication methods. Braz Dent Sci. 2022;25(2):e3000. http://doi.org/10.4322/bds.2022.e3000.

32. Katyal D, Subramanian AK, Venugopal A, Marya A. Assessment of wettability and contact angle of bonding agent with enamel surface etched by five commercially available etchants: an in vitro study. Int J Dent. 2021;2021:9457553. http://doi.org/10.1155/2021/9457553. PMid:34659417.

33. Wege HA, Holgado-Terriza JA, Rosales-Leal JI, Osorio R, Toledano M, Cabrerizo-Vílchez MA. Contact angle hysteresis on dentin surfaces measured with ADSA on drops and bubbles. Colloids Surf A Physicochem Eng Asp. 2002;206(1-3):469-83. http://doi.org/10.1016/S0927-7757(02)00088-2.

34. Yaseen SN, Taqa AA, Al-Khatib AR. The effect of incorporation Nano Cinnamon powder on the shear bond of the orthodontic composite (an in vitro study). J Oral Biol Craniofac Res. 2020;10(2):128-34. http://doi.org/10.1016/j.jobcr.2020.03.008. PMid:32309130.

35. EL-Awady AA, Al-Khalifa HN, Mohamed RE, Ali MM, Abdallah KF, Hosny MM, et al. Shear bond strength and antibacterial efficacy of cinnamon and titanium dioxide nanoparticles incorporated experimental orthodontic adhesive: an in vitro comparative study. Appl Sci. 2023;13(10):6294. http://doi.org/10.3390/app13106294.

36. Gouvêa DB, Santos NM, Pessan JP, Jardim JJ, Rodrigues JA. Enamel subsurface caries-like lesions induced in human teeth by different solutions: a TMR analysis. Braz Dent J. 2020;31(2):157-63. http://doi.org/10.1590/0103-6440202003123. PMid:32556015.

37. Taqa AA, Sulieman RT. Artificial saliva sorption for three different types of dental composite resin: an in vitro study. Al-Rafidain Dent J. 2011;11(3):296-302. http://doi.org/10.33899/rden.2011.164465.

38. Reynolds IR. A review of direct orthodontic bonding. Br J Orthod. 1975;2(3):171-8. http://doi.org/10.1080/03012 28X.1975.11743666.

39. Almeshal R, Pagni S, Ali A, Zoukhri D. Antibacterial activity and shear bond strength of orthodontic adhesive containing various sizes of chitosan nanoparticles: an in vitro study. Cureus. 2024;16(2):e54098. http://doi.org/10.7759/cureus.54098. PMid:38487116.

40. Mohammed RR, Rafeeq RA. Evaluation of the shear bond strength of chitosan nanoparticles-containing orthodontic primer: an in vitro study. Int J Dent. 2023;2023:9246297. http://doi.org/10.1155/2023/9246297. PMid:37577257.

41. Katyal D, Jain RK, Sankar GP, Prasad AS. Antibacterial, cytotoxic, and mechanical characteristics of a novel chitosan-modified orthodontic primer: an: in-vitro: study. J Int Oral Health. 2023;15(3):284-9. http://doi.org/10.4103/jioh.jioh_240_22.

42. Sorourhomayoun S, Alaghehmand H, Mahjoub S, Khafri S, Ghasempour M. Shear bond strength of composite to primary enamel teeth treated with different concentrations and various molecular weights of chitosan. Casp. J. Dent. Res. 2021;10:35-41. http://doi.org/10.22088/cjdr.10.1.35.

43. Xu T, Li X, Wang H, Zheng G, Yu G, Wang H, et al. Polymerization shrinkage kinetics and degree of conversion of resin composites. J Oral Sci. 2020;62(3):275-80. http://doi.org/10.2334/josnusd.19-0157. PMid:32493864.

44. Machado AHS, Garcia IM, Motta ASD, Leitune VCB, Collares FM. Triclosan-loaded chitosan as antibacterial agent for adhesive resin. J Dent. 2019;83:33-9. http://doi.org/10.1016/j.jdent.2019.02.002. PMid:30794843.

45. Putzeys E, Nys S, Cokic SM, Duca RC, Vanoirbeek J, Godderis L, et al. Long-term elution of monomers from resin-based dental composites. Dent Mater. 2019;35(3):477-85. http://doi.org/10.1016/j.dental.2019.01.005. PMid:30704750.

46. Tanaka CB, Lopes DP, Kikuchi LN, Moreira MS, Catalani LH, Braga RR, et al. Development of novel dental restorative composites with dibasic calcium phosphate loaded chitosan fillers. Dent Mater. 2020;36(4):551-9. http://doi.org/10.1016/j.dental.2020.02.004. PMid:32089269.

47. Chanachai S, Chaichana W, Insee K, Benjakul S, Aupaphong V, Panpisut P. Physical/mechanical and antibacterial properties of orthodontic adhesives containing calcium phosphate and nisin. J Funct Biomater. 2021;12(4):73. http://doi.org/10.3390/jfb12040073. PMid:34940552.

48. Mahapoka E, Arirachakaran P, Watthanaphanit A, Rujiravanit R, Poolthong S. Chitosan whiskers from shrimp shells incorporated into dimethacrylate-based dental resin sealant. Dent Mater J. 2012;31(2):273-9. http://doi.org/10.4012/dmj.2011-071. PMid:22447062.

49. Altmann ASP, Collares FM, Balbinot GS, Leitune VCB, Takimi AS, Samuel SMW. Niobium pentoxide phosphate invert glass as a mineralizing agent in an experimental orthodontic adhesive. Angle Orthod. 2017;87(5):759-65. http://doi.org/10.2319/122417-140.1. PMid:28686093.

50. Kauppi MR, Combe EC. Polymerization of orthodontic adhesives using modern high-intensity visible curing lights. Am J Orthod Dentofacial Orthop. 2003;124(3):316-22. http://doi.org/10.1016/S0889-5406(03)00402-5. PMid:12970666.

51. Sionkowska A, Płanecka A, Lewandowska K, Kaczmarek B, Szarszewska P. Influence of UV-irradiation on molecular weight of chitosan. Prog Chem Appl Chitin Deriv. 2013;18:21-8.

52. Tummala M, Rashmi AS, Kundabala M, Chandrasekhar V, Ballal V. Assessment of the wetting behavior of three different root canal sealers on root canal dentin. J. Conserv. Dent. JCD. 2012;15(2):109-12. http://doi.org/10.4103/0972-0707.94573. PMid:22557805.

53. Niu J, Li D, Zhou Z, Zhang J, Liu D, Zhao W, et al. The incorporation of phosphorylated chitosan/amorphous calcium phosphate nanocomplex into an experimental composite resin. Dent Mater J. 2021;40(2):422-30. http://doi.org/10.4012/dmj.2019-427. PMid:33518690.

54. Garcia LGS, Rocha MGD, Freire RS, Nunes PIG, Nunes JVS, Fernandes MR, et al. Chitosan microparticles loaded with essential oils inhibit duo-biofilms of Candida albicans and Streptococcus mutans. J Appl Oral Sci. 2023;31:e20230146. http://doi.org/10.1590/1678-7757-2023-0146. PMid:37729259.

55. Valian A, Goudarzi H, Nasiri MJ, Roshanaei A, Sadeghi Mahounak F. Antibacterial and anti-biofilm effects of chitosan nanoparticles on Streptococcus mutans isolates. J Iran Med Counc. 2023;6:292-8. http://doi.org/10.18502/jimc.v6i2.12238.

56. Yao S, Chen S, Wang R, Zhang K, Lin X, Mai S. Antibacterial activity and bonding performance of carboxymethyl chitosan-containing dental adhesive system. Int J Adhes Adhes. 2022;119:103269. http://doi.org/10.1016/j.ijadhadh.2022.103269.

57. Kikuchi LNT, Freitas SRM, Amorim AF, Delechiave G, Catalani LH, Braga RR, et al. Effects of the crosslinking of chitosan/DCPA particles in the antimicrobial and mechanical properties of dental restorative composites. Dent Mater. 2022;38(9):1482-91. http://doi.org/10.1016/j.dental.2022.06.024. PMid:35835609.

58. Harini B, Rajeshkumar S, Roy A. Biomedical application of chitosan and piper longum-assisted nano zinc oxide-based dental varnish. Appl Biochem Biotechnol. 2022;194(3):1303-9. http://doi.org/10.1007/s12010-021-03712-8. PMid:34677761.

59. Mirhashemi AH, Bahador A, Kassaee MZ, Daryakenari GH, Ahmad Akhondi MS, Sodagar A. Antimicrobial Effect of Nano-Zinc Oxide and Nano-Chitosan Particles in Dental Composite Used in Orthodontics. J Med Bacteriol. 2013;2(3,4):1-10.

60. Alsoufy S, Al-Banaa L, Al-Khatib A. Natural products applications in orthodontics: a review. Al-Rafidain Dent J. 2024;24:499-508.

61. Simeonov M, Gussiyska A, Mironova J, Nikolova D, Apostolov A, Sezanova K, et al. Novel hybrid chitosan/calcium phosphates microgels for remineralization of demineralized enamel: a model study. Eur Polym J. 2019;119:14-21. http://doi.org/10.1016/j.eurpolymj.2019.07.005.

62. Song J, Li T, Gao J, Li C, Jiang S, Zhang X. Building an aprismatic enamel-like layer on a demineralized enamel surface by using carboxymethyl chitosan and lysozyme-encapsulated amorphous calcium phosphate nanogels. J Dent. 2021;107:103599. http://doi.org/10.1016/j.jdent.2021.103599. PMid:33561513.

63. Wahied DM, Ezzeldin N, Abdelnabi A, Othman MS, Abd El Rahman MH. Evaluation of surface properties of two remineralizing agents after modification by chitosan nano particles: an in vitro study. Contemp Clin Dent. 2023;14(4):265-71. http://doi.org/10.4103/ccd.ccd_84_23. PMid:38344165.

64. Chen H, Lv C, Guo L, Ma M, Li X, Lan Z, et al. Surface stability and morphology of calcium phosphate tuned by pH values and lactic acid additives: theoretical and experimental study. ACS Appl Mater Interfaces. 2022;14(4):4836-51. http://doi.org/10.1021/acsami.1c18727. PMid:35043625.

65. Paik Y, Kim MJ, Kim H, Kang S-W, Choi Y-K, Kim Y-I. The effect of biomimetic remineralization of calcium phosphate ion clusters-treated enamel surfaces on bracket shear bond strength. Int J Nanomedicine. 2023;18:4365-79. http://doi.org/10.2147/IJN.S420462. PMid:37545871.

Lara Riyadh Al-Banaa
(Corresponding address)
Mosul University, College of Dentistry, Department of Pedodontics, Orthodontic and Preventive Dentistry, Mosul, Iraq.
Email: dr-lara-ra@uomosul.edu.iq

Date submitted: 2024 Oct 19
Accept submission: 2024 Dec 26